

# Experiments on laser driven beatwave acceleration in a ponderomotively formed plasma channel<sup>a)</sup>

S. Ya. Tochitsky,<sup>1,b)</sup> R. Narang,<sup>1</sup> C. V. Filip,<sup>1</sup> P. Musumeci,<sup>2</sup> C. E. Clayton,<sup>1</sup> R. B. Yoder,<sup>2</sup> K. A. Marsh,<sup>1</sup> J. B. Rosenzweig,<sup>2</sup> C. Pellegrini,<sup>2</sup> and C. Joshi<sup>1</sup>

<sup>1</sup>Neptune Laboratory, Department of Electrical Engineering, University of California, Los Angeles, California 90095

<sup>2</sup>Department of Physics, University of California, Los Angeles, California 90095

(Received 28 October 2003; accepted 21 December 2003; published online 23 April 2004)

A 10 ps long beam of 12 MeV electrons is externally injected into a  $\sim 3$ -cm long plasma beatwave excited in a laser ionized hydrogen gas. The electrons have been accelerated to 50 MeV with a gradient of  $\sim 1.3$  GeV/m. It is shown that when the effective plasma wave amplitude-length product is limited by ionization-induced defocusing (IID), acceleration of electrons is significantly enhanced by using a laser pulse with a duration longer than the time required for ions to move across the laser spot size. Both experiments and two-dimensional simulations reveal that, in this case, self-guiding of the laser pulse in a ponderomotively formed plasma channel occurs. This compensates for IID and drives the beatwave over the longer length compared to when such a channel is not present.

© 2004 American Institute of Physics. [DOI: 10.1063/1.1651100]

## I. INTRODUCTION

A laser-plasma accelerator of particles utilizes a relativistic plasma wave (RPW) driven by a high-power laser beam. The use of a RPW makes it possible to couple energy of a transverse electromagnetic wave of the laser to charged particles via the longitudinal electric field of the electrostatic plasma wave.<sup>1</sup> The past decade has seen great advances in laser-driven RPWs excited by both 1- $\mu\text{m}$  and 10- $\mu\text{m}$  laser pulses.<sup>2</sup> Experiments using the 1- $\mu\text{m}$  laser are typically carried out at high electron plasma density ( $n_e$ ) of  $\sim 10^{19} \text{ cm}^{-3}$  resulting in extremely high,  $>100$  GeV/m accelerating gradients.<sup>3</sup> On the other hand experiments with 10- $\mu\text{m}$  lasers are typically carried out at much lower  $n_e$  of  $\sim 10^{16} \text{ cm}^{-3}$  where gradients are in the range 1–3 GeV/m.<sup>4</sup> These values are orders of magnitude higher than those for conventional radio-frequency devices. In spite of the demonstrated high gradients, the potential of laser-plasma accelerators for the next-generation of particle accelerators cannot be ascertained without solving the issue of matching of a particle beam into the plasma accelerating structure and efficient extraction of this beam from such a structure. This is important for optimizing the energy extraction efficiency (beam loading) as well as for staging these plasma-based structures. To study these issues a beam of electrons has to be injected into a plasma accelerator. Most of the experiments to date have been on the acceleration of self-trapped electrons and much less attention has been paid to the external injection of the particle beam in the plasma accelerating structure.<sup>4,5</sup>

In the Neptune Laboratory at UCLA we have begun to address the issues of beam loading by injecting a well-characterized electron beam into a preformed plasma accelerating structure and exploring methods for extracting a

high-quality beam. In this paper we present our findings to date. Here, a two-wavelength laser pulse (frequencies  $\omega_1, \omega_2$ ) of a TW CO<sub>2</sub> laser system resonantly drives a longitudinal RPW of frequency  $\omega_p \approx \Delta\omega \equiv \omega_1 - \omega_2$ , where  $\omega_p = (4\pi n_e e^2/m)^{1/2}$ . This plasma beatwave acceleration (PBWA) scheme<sup>1,4</sup> allows the excitation of a robust RPW structure without the need to have either extremely short and intense laser pulses as in the laser-wakefield accelerator or extremely intense laser pulses in combination with a high plasma density as in the self-modulated laser-wakefield accelerator. Furthermore such a slowly driven RPW are relatively long lived simplifying its synchronization with an externally injected electron bunch. In these experiments the externally injected electron bunch, with a duration shorter than the RPW's envelope, are deterministically synchronized with the RPW but not optimally coupled into it.

For efficient injection and extraction of a high quality beam the ideal accelerating field structure would be a one-dimensional wave with transversely uniform accelerating fields and minimum focusing/defocusing forces.<sup>6</sup> This requires a laser focal spot of a diameter  $2w_0$  larger than the plasma wavelength  $\lambda_p = 2\pi c/\omega_p$ . Increasing the spot size increases the Rayleigh range  $Z_R = \pi w_0^2/\lambda$ , where  $\lambda$  is the laser wavelength, and therefore the interaction length between the electrons and the RPW. However, if the laser itself creates the plasma,  $Z_R$  is limited by ionization-induced defocusing (IID) of the laser beam.<sup>7</sup> This defocusing is caused by a radial gradient in the refractive index resulting from the faster ionization of the gas on axis of the laser beam. In a static filled chamber the maximum  $Z_{R,\text{max}}$  at which IID becomes a limiting factor can be estimated for a desired electron density by

$$Z_{R,\text{max}} \approx n_{\text{cr}} \lambda / n_e, \quad (1)$$

where  $n_{\text{cr}}$  is the critical density for which the plasma frequency equals the laser frequency. According to Eq. (1),

<sup>a)</sup>Paper LI2 1, Bull. Am. Phys. Soc. **48**, 199 (2003).

<sup>b)</sup>Invited speaker.

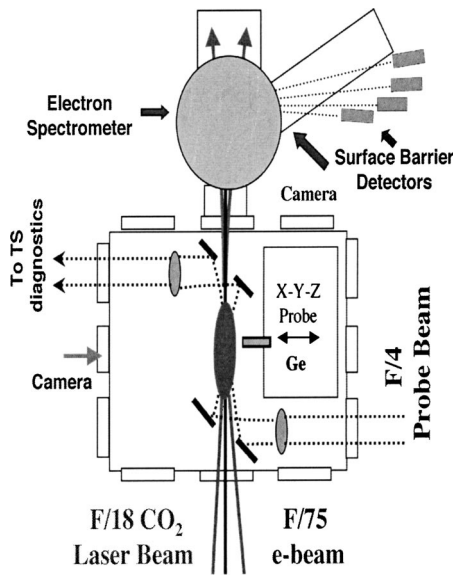


FIG. 1. Schematic of the experimental set-up.

there is a maximum  $Z_R$  and, therefore, a maximum  $w_0$  above which the laser intensity achieved at the focal region will be significantly reduced because of IID. Control and optimization of the coupling of laser light to RPWs in laser-ionized plasmas, for which these refraction effects become important, is one of the main challenges for plasma accelerators.

In this paper we report PBWA of externally injected electrons in a several-centimeter long plasma when  $2w_0 > \lambda_p$  and the length of the RPW excitation is restricted by IID. It is shown that the interaction length and therefore energy gained by particles is enhanced significantly by using an asymmetric (fast front and slow fall) laser pulse. The duration of the pulse should be longer than the characteristic time for ions to move transversely a distance equal to  $w_0$  given by

$$\Delta t_i = \frac{2\pi w_0 c}{e} \sqrt{\frac{m_e m_i \epsilon_0 c}{2I \lambda^2}}, \quad (2)$$

where  $m_i$  the ion mass and  $I$  is the laser intensity.<sup>8</sup> In this case the laser pulse is self-guided in a ponderomotively formed plasma channel. Guiding compensates for the IID and efficiently drives the beatwave over the longer length compared to the case when such a channel is not present. The experimentally observed phenomena of IID induced focal shift, time integrated length of RPW and the output electron spectrum are all found to be in a qualitative agreement with modelling the experiments using a 2D code.

## II. EXPERIMENTAL SET-UP

The layout of the PBWA experiment is shown in Fig. 1. A TW, two-wavelength CO<sub>2</sub> laser system, producing 100–400 ps long pulses at 10.3  $\mu\text{m}$  and 10.6  $\mu\text{m}$ , was used to drive the plasma beatwave.<sup>9</sup> This pair of lines determined the value of the resonant electron plasma density of  $n_e \approx 9.4 \times 10^{15} \text{ cm}^{-3}$  ( $\lambda_p = 340 \mu\text{m}$ ). For this resonant plasma density, using Eq. (1), we find that IID becomes significant for  $Z_R \geq 11 \text{ mm}$ . The laser beam was focused by an F/18 lens

giving a  $1/e^2$  intensity focal spot diameter  $2w_0 \approx 400 \mu\text{m}$  and a Rayleigh range of  $2Z_R \approx 26 \text{ mm}$ . A 10-ps full width at half maximum (FWHM) electron bunch produced by an rf photoinjector<sup>10</sup> was externally injected in the plasma accelerating structure. A 12 MeV electron beam with an energy spread of  $\sim 0.5\%$  was focused down to  $150 \mu\text{m}$  ( $\sigma_{\text{rms}}$ ) at the laser focal plane in a vacuum. The two beams were precisely overlapped in space with a residual angular misalignment of  $0.1^\circ$ – $0.2^\circ$ . Typically  $3 \times 10^8$  particles were injected into the plasma produced in a vacuum chamber filled with hydrogen gas. The energy spectrum of the electron beam was analyzed using a Browne–Buechner spectrometer in combination with a fluorescer screen (for energies  $12 < E < 15 \text{ MeV}$ ) and a set of five 1-mm thick Si surface barrier detectors (SBDs) (for energies  $E > 15 \text{ MeV}$ ). With the current set-up 3–5 electrons with maximum energy up to 50 MeV were detectable.

One of the main difficulties of measuring ionizing radiation (electrons in particular) is that the SBDs are sensitive to a variety of radiation sources. To decrease the background caused by stray hard x rays produced by bremsstrahlung, each SBD was placed in a thick lead housing with an aperture equal to 8 mm (detector size). Detectors were also shielded by 1–3 mm of Cu cutting off all x rays below 0.1 MeV at the peak of SBD's sensitivity. Note that measurements using lead attenuators revealed that residual noise is dominated by hard x rays in the range of 0.3–2 MeV. A series of null tests were performed under various conditions, which could, in principle, produce false signals on our detectors. They included the transverse blowing of the e-beam by the laser beam or plasma producing scattered 12 MeV electrons, acceleration of electrons by a Raman instability in the plasma rather than the beatwave, and the acceleration of background plasma electrons rather than the injected electrons from the photoinjector. All null tests using both single- and two-wavelength laser pulses confirmed that the signal detected above the noise is a result of acceleration of the injected electrons by the RPW.

The optical diagnostics used in the experiment were a charge-coupled device (CCD) camera for the plasma fluorescence images and collective Thomson scattering of a 0.53- $\mu\text{m}$  probe beam. As shown in Fig. 1, two flat mirrors with holes were utilized to send the F/4 focused 0.53- $\mu\text{m}$  beam collinearly through the plasma. Given the small interaction length of approximately 1 mm compared to the length of the plasma, we were able to map the longitudinal variation of the RPW's amplitude by scanning the sampling point. This collinear Thomson scattering diagnostic system allowed us to resolve the scattered signal both in time and frequency.<sup>11</sup>

In order to inject a 10-ps electron bunch (FWHM) at the very maximum of the plasma wave in time, a CO<sub>2</sub> laser pulse and electrons must be synchronized on a picosecond time scale. Synchronization is possible because the same 1- $\mu\text{m}$  pulse is used to produce electrons on a photocathode and to switch a short 10- $\mu\text{m}$  pulse for amplification in a master oscillator-power amplifier CO<sub>2</sub> laser system.<sup>9</sup> A two-step technique was used for synchronization; the cross-correlation between 10- $\mu\text{m}$  photons and electrons measured

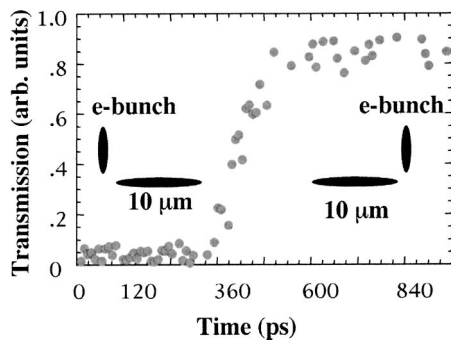


FIG. 2. The transmitted signal at  $10\ \mu\text{m}$  as a function of the delay between the laser pulse and the electron bunch.

with an unamplified laser pulse was followed by the compensation for a constant time delay gained in the active medium of the final  $\text{CO}_2$  amplifier.

Electron-beam-controlled transmission of  $10\text{-}\mu\text{m}$  radiation in Ge (Ref. 12) was utilized for the cross-correlation measurement. For this purpose the pulse was sent through a 2-mm thick germanium plate at the laser focus and the time dependence of the  $10\text{-}\mu\text{m}$  transmission was recorded. The latter was realized by a computer controlled optical delay line. A typical result of cross-correlation measurement is presented in Fig. 2. If the electrons reach the Ge plate before the  $\text{CO}_2$  laser pulse, the  $10\text{-}\mu\text{m}$  radiation is fully attenuated by the free carriers generated by the electron beam. This is seen to be the case from 0 to 340 ps in Fig. 2. From 340 to approximately 600 ps the electron bunch and the  $10\text{-}\mu\text{m}$  pulse cross each other, resulting in the increase of transmission or cross-correlation. The plasma formation in a semiconductor happens on a time scale similar to the duration of the plasma creating electron bunch. Therefore, accuracy of the cross-correlation measurements is limited by the 10-ps bunch length. Note that for the latter to be true the spot size for the electron beam should be larger than that for the laser beam. As seen in Fig. 2, a total width of the cross-correlation curve is  $\sim 260$  ps, which agrees very well with a  $\text{CO}_2$  laser pulse length measured by a streak camera.

The cross-correlation measurements were conducted with an unamplified laser pulse propagating through a final, triple passed, 2.5-m long multiatmosphere  $\text{CO}_2$  amplifier<sup>9</sup> with no inversion of population. It is known that the resonant behavior of the refractive index ( $n$ ) in the vicinity of a homogeneously broadened molecular transition results in an increase of  $n$  in the inverted medium.<sup>13</sup> This, along with the pressure-shift-caused frequency off-set between laser lines in the master oscillator and the final amplifier,<sup>14</sup> lead to decrease of the group velocity of the laser pulse within the inverted medium of the final amplifier in comparison with no-gain conditions. A series of measurements using a streak camera revealed that a  $120 \pm 20$  ps pulse delay was gained in our case. Therefore in the experiment we compensated for the delay after the cross-correlation measurement. Thus a total uncertainty of 20 ps is achieved in synchronization of  $\text{CO}_2$  laser pulses and electron bunches, which was adequate for this experiment.

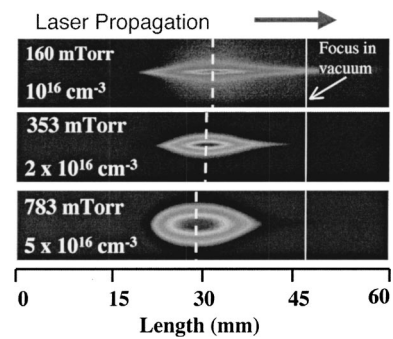


FIG. 3. Fluorescence images of hydrogen plasmas produced by a two-wavelength  $\text{CO}_2$  laser pulse at different pressures 160 mTorr, 353 mTorr, and 783 mTorr demonstrating ionization-induced defocusing of the laser beam. Dashed white lines indicate the position of the most intense fluorescence in gas—a backfill focus.

### III. EXPERIMENTAL RESULTS

Figure 3 shows fluorescence images from plasmas in  $\text{H}_2$  for different gas pressures around the resonant pressure for RPW excitation. Note that with fully ionized  $\text{H}_2$ , changing the gas pressure is equivalent to varying the plasma density; a fact confirmed by frequency shift measurement of the Raman scattered plasmons.<sup>15</sup> The incident laser power is  $\sim 0.7$  TW for 160 ps pulses. It appears that all the plasmas are asymmetric about the focus in vacuum and the maximum emission of light (backfill focus) is located upstream of the vacuum focus at a distance larger than  $Z_R$ . The backfill focus shifts further upstream when the plasma density is increased from  $10^{16}\text{ cm}^{-3}$  to  $5 \times 10^{16}\text{ cm}^{-3}$ . All the data present compelling evidence that around the resonant plasma density of  $\sim 10^{16}\text{ cm}^{-3}$  the plasma length is limited by IID.

To study the possibility of self-guiding of the laser beam with a subsequent increase in the interaction length beyond that limited by IID, we compared two types of pulses: a short pulse (SP) and a long pulse (LP). The rise time for both pulses was approximately 80 ps, providing the same ionization rate and therefore IID contribution. The peak power of the laser pulse for both SPs and LPs was chosen to be  $\sim 0.5$  TW, corresponding to a vacuum intensity of  $4 \times 10^{14}\text{ W/cm}^2$ . However, in a backfill of  $\text{H}_2$  the maximum laser intensity was limited by IID to approximately twice the field ionization threshold for  $\text{H}_2$ .<sup>7</sup> For the highest intensity achievable in a backfill of  $\text{H}_2 \sim 2 \times 10^{14}\text{ W/cm}^2$  and  $w_0 = 200\ \mu\text{m}$ , the characteristic time  $\Delta t_i$  according to Eq. (2) is 217 ps. The SP, with a duration  $\sim 160$  ps (FWHM) was chosen to be shorter than  $\Delta t_i$ ; the LP had a duration  $\sim 400$  ps, i.e., longer than  $\Delta t_i$ . This allowed direct comparison of the interaction length and the energy gained by electrons with (LP) and without (SP) significant transverse motion of the ions.

Figure 4(a) shows lineouts of three plasma fluorescence images for the two-wavelength SP (curve 1), the single-wavelength LP (curve 2), and the two-wavelength LP (curve 3). All the curves are asymmetric about the focus in vacuum because of IID, with the backfill focus shifted upstream by a distance of  $\sim 13$  mm. Although the full extent of the SP-produced plasma appears to be  $\sim 30$  mm, collinear Thomson

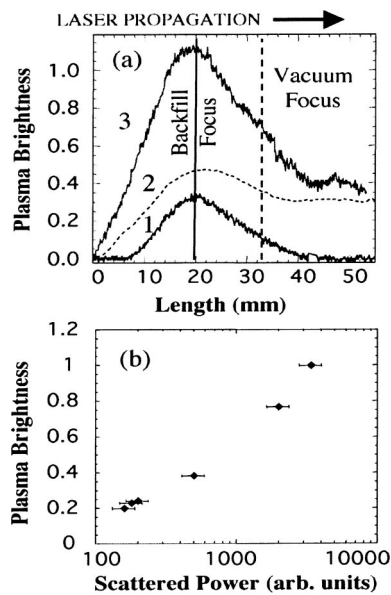


FIG. 4. (a) Lineout of fluorescence images of hydrogen plasmas at 165 mTorr after subtracting the background for a two-wavelength short (1), single-wavelength long (2), and two-wavelength long (3) pulses. (b) Plasma brightness as a function of power of a  $0.53\text{-}\mu\text{m}$  laser beam scattered from the RPW measured by a Thomson scattering diagnostic.

scattering showed that a RPW of significant amplitude,  $\epsilon = \delta n/n_e \approx 0.1$ , where  $\delta n$  is the magnitude of the perturbation of the electron density associated with the RPW, occurred only over  $\geq 10$  mm around the backfill focus. The amount of Thomson scattered light and the deduced value of the wave amplitude dropped rapidly outside this region, presumably due to IID caused longitudinal variations of  $n_e$ . The LP-produced plasmas are brighter in fluorescence and extend over 50 mm in length. Plasma brightness is directly related to the amount of energy stored in it. One reason for the enhanced fluorescence for the LP case is that the modest heating of the plasma by the laser pulse now occurs over a longer time resulting in more recombination emission in these time-integrated images. However, the two-wavelength LP plasma (curve 3) is  $\geq 2\times$  brighter than the one-wavelength LP one (curve 2) over  $\sim 30$  mm. We also recorded, as shown in Fig. 4(b), a strong correlation between the plasma brightness for two-wavelength shots and the amount of light scattered by the RPW measured by a Thomson scattering technique. This points to an additional plasma heating mechanism due to coupling energy of the laser field to a RPW, the magnitude of which increases with the RPW's amplitude (or the measured scattered power). A similar effect has been observed previously in measurements of the x-ray plasma emission from single- and two-wavelength shots taken at resonant densities, where it was deduced that the presence of the RPW additionally increased heating of the plasma electrons from 100 eV to 1 keV.<sup>16</sup>

To distinguish between simple laser heating and laser heating combined with the RPW heating, we plot the peak fluorescence brightness for the LPs as a function of gas pressure as shown in Fig. 5(a). We see that the plasma brightness of one-wavelength shots (dashed line) is similar to that of two-wavelength shots (circles) except for pressures in the

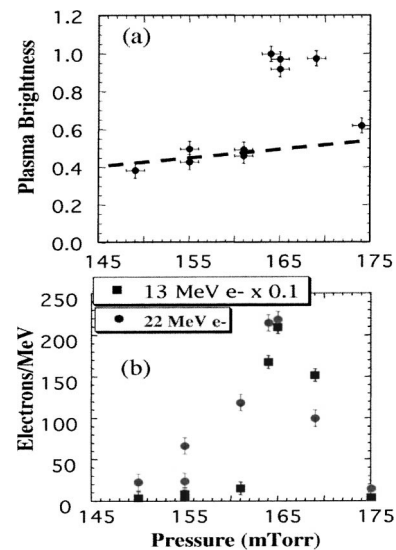


FIG. 5. (a) Plasma brightness as a function of hydrogen pressure for two-wavelength (circles) and single-wavelength (dashed line) long pulses. (b) Number of electrons as a function of hydrogen pressure measured both by a phosphor screen at 13 MeV (squares) and the SBD at 22 MeV (circles).

range of 160–170 mTorr. To confirm that this sharp, factor of 2 increase is due to the excitation of the RPW, we simultaneously measured the pressure dependence of the number of accelerated electrons. In Fig. 5(b) we plot the number of electrons detected both on a phosphor screen (energy 13 MeV) and on the 22 MeV SBD. These also peak at an apparent resonant pressure of 165 mTorr. Thus the observed increase in the plasma brightness in Fig. 5(a) does indeed occur because of the RPW existence, a fact independently confirmed by Thomson scattering measurements. This suggests that increase of greater than factor of 2 between curves 2 and 3 in Fig. 4(a) observed at 165 mTorr of  $\text{H}_2$  is due to the presence of a RPW. From these observations, we can infer that, for a two-wavelength LP an effective length of the RPW (integrated over time) is probably  $\sim 30$  mm. We note that the apparent resonant pressure of 165 mTorr in Fig. 5(b) is  $\sim 15\%$  higher than the theoretical resonant pressure of 143 mTorr calculated for the given pair of  $\text{CO}_2$  lines.<sup>4</sup>

To study its evolution in time, the RPW was probed collinearly by a 10-ps (FWHM), 12 MeV electron bunch. By analyzing signals on SBDs placed at 22 and 27 MeV as a function of the relative time between the laser pulse and the electron bunch, the temporal dynamics of the longitudinal electric field of the RPW (integrated along the electron trajectory) was measured. The results of these measurements at the resonant pressure are shown in Fig. 6(a) along with pulse profiles for both the SP and LP. For the SPs, the signal on the 22 MeV SBD (circles) peaked when electrons were injected at the maximum of the  $\text{CO}_2$  laser pulse, while the 27 MeV SBD did not show any signal at all. When the LPs were used, the number of 22 MeV electrons (triangles) increased by a factor of 4 and 27 MeV electrons (squares) were detected. However this enhanced acceleration occurs not at the peak of the  $\text{CO}_2$  laser pulse but after an additional time delay of approximately 250 ps from the start of the pulse, as can be seen in Fig. 6(a). This time delay is consistent with the esti-

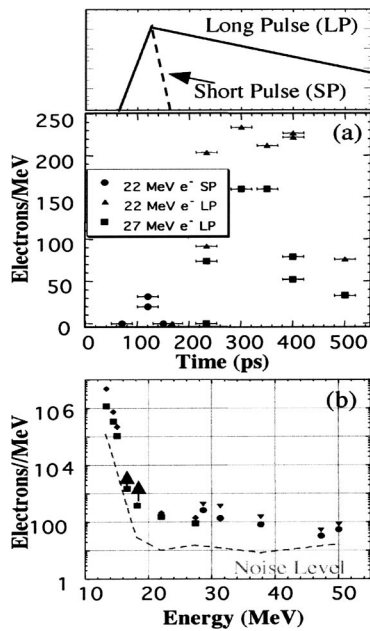


FIG. 6. (a) The schematic pulse profiles for a short pulse (SP) and a long pulse (LP); and time dependence of number of accelerated electrons obtained using SPs at 22 MeV (circles), and those obtained using LPs at 22 MeV (triangles) and 27 MeV (squares). (b) Spectra of electrons accelerated by a LP-driven plasma beatwave. The injection energy is 12 MeV; the black arrows indicate the saturation of detector’s amplifier.

mated  $\Delta t_i$  for our parameters. Another observation in the experiment is that the LP-excited RPW has a long ( $\sim 100$  ps) time window for optimal external injection of particles.

After optimizing the injection time for an electron beam, we recorded single-shot spectra of accelerated electrons. Since in the experiment both transverse and longitudinal sizes of the e-beam were larger than the spot size and the wavelength of the RPW, a continuous electron energy spread was obtained. When the beatwave was driven by a SP, the maximum energy gain  $W_{\max}$  did not exceed 10 MeV. Recall that the diameter of the laser beam was larger than the plasma wavelength of  $340 \mu\text{m}$ . Thus it is valid to use the one dimensional formalism for  $W_{\max} = 0.96\epsilon n_e^{0.5} L$  and the wave amplitude  $\epsilon$  can be estimated. For a length  $L = 10$  mm and the observed  $W_{\max} = 10$  MeV, we obtain  $\epsilon \sim 0.1$ , which is in good agreement with the value obtained from the Thomson scattering measurements.

The electron spectrum for LPs, recorded using two different settings for the magnetic field in the spectrometer: the low-energy side (12–25 MeV) at 0.4 T and the high-energy side (27–50 MeV) at 0.7 T, is shown in Fig. 6(b). We see an experimental spectrum that falls off rapidly away from 12 MeV and extends out to 50 MeV. The total number of accelerated electrons in this case was  $3 \times 10^6$  or  $\geq 1\%$  of the injected number of particles. The flatness of the spectrum from 22 MeV to 50 MeV is believed to be due to the small observation angle (a  $f/75$  cone). As a result we detected only electrons with an emittance of about 10 mm-mrad which is comparable with the emittance of the injected e-beam. The maximum electron energy gives an upper bound on the longitudinal electric field of the wave integrated along the electron trajectory through the wave. The energy gain of 38 MeV

demonstrates that for LPs there is a significant enhancement in the energy gain compared to SPs at the same power.

Summarizing the experimental data we note the following: The plasma beatwave length-amplitude product is 3.8 times larger for the LPs in comparison to the SPs. The obtained enhancement in the energy gain is consistent with the observed increase in the effective length of RPW deduced in connection with Fig. 4(a). Figure 4(a) also shows that for LPs the plasma length increased downstream from the backfill focus. The maximum energy gain for LPs in Fig. 6(a) is reached after a 250 ps delay from the start of the laser pulse which is larger than  $\Delta t_i$ . The measured optimal pressure for acceleration, as seen in Fig. 5(b), is approximately 15% higher than one needed for a RPW excitation.

Thus in the experiment the apparent resonant pressure is too high for resonant excitation of a RPW. Therefore for the RPW to exist the initial plasma density somewhere must be depressed. The transverse ponderomotive force of the laser field can bring the density down to the resonant density on the hydrodynamic time scale  $\Delta t_i$ . For SPs this may result only in excitation of the wave around the backfill focus where the intensity is the highest and, therefore the ponderomotive plasma blow-out is the largest. However, for the much longer LPs, this ponderomotively induced on-axis density depression  $\Delta n_e \approx 15\%$  can guide a laser beam at the backfill focus, compensate for IID, feed energy to the downstream region causing further ionization and increase the RPW length. Using the channel guiding condition,<sup>17</sup>  $\Delta n_e = (r_0 \pi w_{\text{ch}}^2)^{-1}$ , where  $w_{\text{ch}}$  is the radius of a parabolic channel and  $r_0$  is the classical electron radius, we obtain  $w_{\text{ch}} = 282 \mu\text{m}$ , a value that is close to the backfill focus spot size and therefore the laser beam can be guided. Hence, after the 250-ps delay the plasma density in the channel is close to resonant for driving of the RPW and channel-enhanced acceleration of electrons. Note that similar self-guiding of a part of a long 1- $\mu\text{m}$  pulse in a ponderomotively formed plasma channel has been reported for a laser intensity of  $10^{16} \text{ W/cm}^2$ .<sup>18</sup> To gain insight into all these complicated processes in the plasma, we modelled ionization, refraction, channel formation, and excitation of the RPW for parameters close to those in the experiment.

#### IV. SIMULATIONS

The excitation of several-centimeter-long RPWs and injection of electrons into plasma beatwave were simulated using the two-dimensional (2D) slab, particle-in-cell (PIC) code TURBOWAVE.<sup>19</sup> We note that self-focusing and diffraction evolve somewhat differently in 2D codes with cylindrical versus slab geometry. However, as will be shown below the ponderomotive guiding center approximation used in TURBOWAVE, which allows to model the space (a 4-cm long plasma) and time (100 s of ps) scales used in the experiment, is adequate for qualitative analysis of the plasma channel related physics.

In simulations a two-wavelength (10.59 and 10.27  $\mu\text{m}$ ) beam was focused to a spot size of  $200 \mu\text{m}$  at the center of a  $43 \text{ mm} \times 2.5 \text{ mm}$  computational box. The laser pulse had an 80-ps risetime followed by a constant intensity of

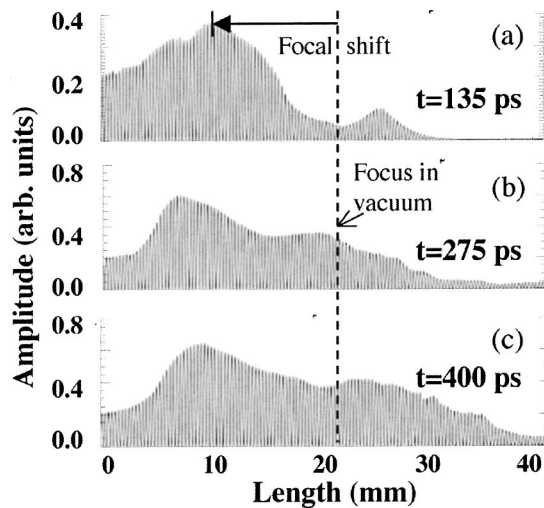


FIG. 7. Horizontal lineouts of the calculated laser field amplitude on axis (a) at 135 ps, (b) 275 ps, and (c) 400 ps from the start of the laser pulse.

$4 \times 10^{14}$  W/cm<sup>2</sup> which lasted for 400 ps. This pulse profile allowed to study the plasma dynamics for both the SP and LP regimes. The initial gas pressure was set to be 10% above the theoretical value of the resonant pressure.

In Fig. 7 we present on-axis, horizontal lineouts of the laser field amplitude for time  $t = 135$  ps (a), 275 ps (b), and 400 ps (c) from the beginning of the laser pulse. For all three snapshots in Fig. 7 there is an IID-caused upstream shift of the backfill focus relative to the value observed in the experiment. As seen in Fig. 7(a), at  $t = 135$  ps ( $t < \Delta t_i$ ), refractive losses limit the region of a high laser amplitude to the upstream region of the vacuum focus. At  $t = 135$  ps, it appears that the laser amplitude at the upstream boundary does not go to zero but this is only because the laser intensity in the simulations is held constant after the peak intensity is reached, whereas in the experiment it falls. However, later in time, at  $t > \Delta t_i$ , more laser power is delivered downstream, reaching the end of a computational box at  $t = 400$  ps. Moreover, the peak laser intensity in Figs. 7(b) and 7(c) also grows as a result of decreasing the spot size. These data clearly indicate a self-guiding process initiated on the hydrodynamic time scale  $\Delta t_i$ . This correlates very well with the increase in the plasma length shown in Fig. 8 for the same three time windows as in Fig. 7. At  $t = 135$  ps length of fully ionized H<sub>2</sub> is approximately 17 mm. Actually at  $t = 80$  ps, which is at the peak of the laser pulse (not shown), the fully ionized region is almost exactly this length. The plasma length increases to 30 mm and almost 40 mm for  $t = 275$  ps and  $t = 400$  ps, respectively. The electron density channel produced for  $t > \Delta t_i$  is clearly seen in Figs. 8(b) and 8(c).

These simulations show that, for  $t < \Delta t_i$ , IID causes a significant loss of laser intensity limiting the plasma formation to the upstream region of the vacuum focus. Later in time, a small electron density gradient produced by the ponderomotive force of the laser results in space-charge separation, and ions slowly drift out of the central area of the laser beam due to this space-charge field, pulling more electrons behind them. As a result of this multistep process in the

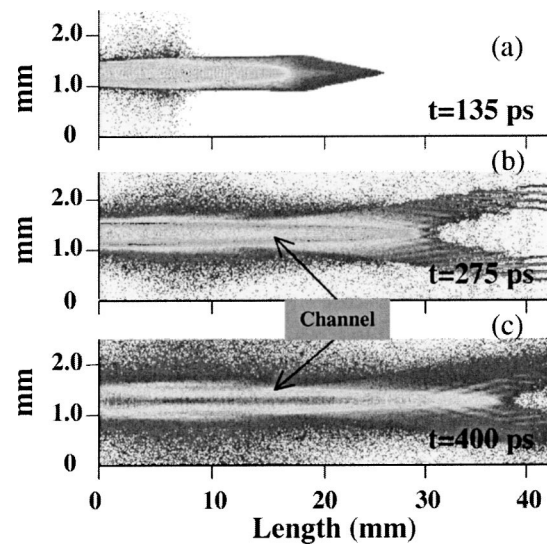


FIG. 8. Calculated electron density distribution (a) at 135 ps, (b) 275 ps, and (c) 400 ps from the start of the laser pulse.

plasma, a macroscopic channel is formed and self-guiding of the laser beam is initiated. Guiding in the plasma channel compensates for IID and delivers laser power further downstream creating a longer plasma. As the plasma density is ponderomotively reduced to the resonant value, the RPW is excited and the channel formation is enhanced by the ponderomotive force of the plasma beatwave.<sup>20</sup>

In Fig. 9 we present the temporal evolution of the RPW. At  $t = 135$  ps the RPW with a normalized amplitude of  $\sim 0.25$  is localized from 0 to 15 mm in the simulation box. At this time, when the plasma wave amplitude is maximum, we injected approximately 1500 test electrons. The test electron

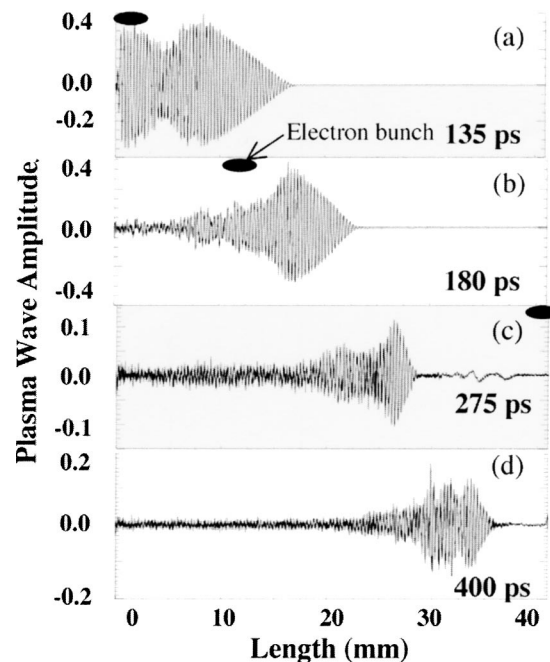


FIG. 9. Horizontal lineouts of the calculated normalized plasma wave amplitude on the axis of laser beam (a) at 135 ps, (b) 180 ps, (c) 275 ps, and (d) 400 ps from the start of the laser pulse.

bunch had a duration of 2 ps (FWHM) and zero transverse emittance. At  $t=180$  ps guiding of the  $10\text{-}\mu\text{m}$  beam in the plasma channel, produced by the combined effects of the ponderomotive forces of the laser and the RPW, minimizes the effect of IID. This feeds more power downstream and results in a downstream motion of the density region where the plasma density is resonant and the RPW is excited. This laser hole boring,<sup>18</sup> as shown in Fig. 9(d), tends to continue until the end of the computational box with a speed decreasing from  $\sim 0.5c$  ( $t=180$  ps) to  $\sim 0.35c$  ( $t=275$  ps). However, because of the ponderomotive transverse drift of ions, the plasma density in the upstream region drops below the resonant value limiting the length of the RPW at any instant in the channel to 12–15 mm. Recall that the transit time of the electrons across the box is 140 ps. Therefore an electron injected in this channel at  $t=135$  ps overtakes the RPW [as seen in Fig. 9(c)] and, therefore sample the RPW over an effective interaction length approaching 25–27 mm. For these conditions, test electrons gained up to 38 MeV which is in a good agreement with the experiment. Furthermore, as the test electrons exited the plasma channel they were strongly defocused because of the termination of the confining electric field of the RPW itself and that of the excess ion density in the channel. These transverse effects may explain the small number of electrons with  $E > 22$  MeV detected in the experiment.

These simulations have qualitatively confirmed many features seen in the experiment and give insight to physics behind the observed effects. The enhancement in the energy gain for the LP- in comparison with the SP-driven PBWA is the result of an increase in the interaction length caused by self-guiding of the laser beam in a ponderomotively formed plasma channel. The experimentally observed optimal time delay for reaching the maximum energy gain (as well as excess initial plasma density) is related to a time necessary for a deep enough channel to form. This injection time provides the maximum longitudinal electric field integrated along the electron trajectory through the moving downstream envelope of the RPW. The RPW in the channel exists over several hundred picoseconds and the dynamics of the large amplitude plasma beatwave is dominated by the longitudinal variation of the electron density.

## V. SUMMARY

We have demonstrated the acceleration of an externally injected 10-ps electron bunch deterministically synchronized with a RPW excited by the laser beatwave mechanism. By increasing the laser beam spot size ( $2w_0 > \lambda_p$ ) we produced a quasi-1D accelerating structure with a longitudinal electric field much higher than the radial electric field. We have shown that for this case, when the interaction length is limited by IID, using laser pulses with durations longer than the characteristic time of ion motion  $\Delta t_i$  initiates a self-guiding process in a ponderomotively formed plasma channel. Guiding compensates for IID and results in a  $\sim 3$ -cm long interaction length for a laser-driven plasma device with a  $\sim 1$  GeV/m acceleration gradient. Channel-assisted PBWA has

increased the energy gain by a factor of 3.8 (from 10 to 38 MeV) in comparison with the case when laser pulses of the same power are shorter than  $\Delta t_i$ . This energy gain enhancement is in good agreement with that obtained in 2D simulations. Although the energy gain for such a plasma-channel-assisted acceleration is substantially larger, only about 1% of the total injected particles are seen to exit with approximately the same emittance as that for the injected beam. The throughput can be increased from the present level to  $\sim 10\%$  level by using an electron beam that has much smaller spot size than the RPW. We are currently exploring whether injection of such a tightly focused and, ultimately, a longitudinally prebunched (at the period of the RPW) electron beam will lead to a better beam quality and throughput in the future experiments.

## ACKNOWLEDGMENTS

The authors would like to thank W. B. Mori and D. F. Gordon for useful discussions.

This work was supported by the DOE Contract No. DE-FG03-92ER40727.

- <sup>1</sup>T. Tajima and J. M. Dawson, *Phys. Rev. Lett.* **43**, 267 (1979).
- <sup>2</sup>*Handbook of Accelerator Physics and Engineering*, edited by A. Chao and M. Tigner (World Scientific, Singapore, 1999).
- <sup>3</sup>A. Modena, Z. Najmudin, A. E. Dangor *et al.*, *Nature (London)* **377**, 606 (1995); D. Umstadter, S.-Y. Chen, A. Maksimchuk, G. Mourou, and R. Wagner, *Science* **273**, 472 (1996); A. Ting, C. I. Moore, K. Krushelnik *et al.*, *Phys. Plasmas* **4**, 1889 (1997); W. P. Leemans, D. Rodgers, P. E. Catravas *et al.*, *ibid.* **8**, 2510 (2001); V. Malka, S. Fritzler, E. Lefebvre *et al.*, *Science* **298**, 1596 (2002).
- <sup>4</sup>C. E. Clayton, K. A. Marsh, A. Dyson, M. Everett, A. Lal, W. P. Leemans, R. Williams, and C. Joshi, *Phys. Rev. Lett.* **70**, 37 (1993).
- <sup>5</sup>F. Dorchies, F. Amiranoff, V. Malka *et al.*, *Phys. Plasmas* **6**, 2903 (1999).
- <sup>6</sup>T. Katsouleas, S. Wilks, P. Chen, J. M. Dawson, and J. J. Su, *Part. Accel.* **22**, 81 (1987).
- <sup>7</sup>W. P. Leemans, C. E. Clayton, W. B. Mori, P. K. Kaw, A. Dyson, C. Joshi, and J. M. Wallace, *Phys. Rev. A* **46**, 1091 (1992); P. Monot, T. Augustie, L. A. Lompre, G. Mainfray, and C. Manus, *J. Opt. Soc. Am. B* **9**, 1579 (1992).
- <sup>8</sup>P. Gibbon, F. Jakober, P. Monot, and T. Augustie, *IEEE Trans. Plasma Sci.* **24**, 343 (1996).
- <sup>9</sup>S. Ya. Tochitsky, R. Narang, C. Filip, C. E. Clayton, K. A. Marsh, and C. Joshi, *Opt. Lett.* **24**, 1717 (1999).
- <sup>10</sup>S. G. Anderson, M. Loh, P. Musumeci, J. B. Rosenzweig, H. Suk, and M. C. Thompson, in *Advanced Acceleration Concepts, 2000*, edited by P. L. Colestock and S. Kelley (American Institute of Physics, New York, 2000), AIP Conf. Proc. Vol. 569, p. 487.
- <sup>11</sup>C. V. Filip, S. Ya. Tochitsky, R. Narang, C. E. Clayton, K. A. Marsh, and C. Joshi, *Rev. Sci. Instrum.* **74**, 3576 (2003).
- <sup>12</sup>P. B. Corkum, A. J. Alcock, and K. E. Leopold, *J. Appl. Phys.* **50**, 3079 (1979).
- <sup>13</sup>G. T. Schappert and M. J. Herbst, *Appl. Phys. Lett.* **26**, 314 (1975).
- <sup>14</sup>R. C. Hollins and D. L. Jordan, *J. Phys. B* **15**, L491 (1982).
- <sup>15</sup>R. Narang, C. Filip, S. Ya. Tochitsky, D. F. Gordon, C. E. Clayton, K. A. Marsh, and C. Joshi, in *Proceedings of the Particle Accelerator Conference*, Chicago, IL, 2001, edited by P. Lucas and S. Webber (IEEE Operation Center, Piscataway, NJ, 2001), Vol. 5, p. 3996.
- <sup>16</sup>A. K. Lal, D. Gordon, K. Wharton *et al.*, *Phys. Plasmas* **4**, 1434 (1997).
- <sup>17</sup>C. D. Durfee III, J. Lynch, and H. M. Milchberg, *Phys. Rev. E* **51**, 2368 (1995).
- <sup>18</sup>P. E. Young, M. E. Foord, J. H. Hammer, W. R. Kruer, M. Tabak, and S. C. Wilks, *Phys. Rev. Lett.* **75**, 1082 (1995).
- <sup>19</sup>D. F. Gordon, W. B. Mori, and T. Antonsen, *IEEE Trans. Plasma Sci.* **28**, 1135 (2000).
- <sup>20</sup>C. Joshi, C. Clayton, and F. Chen, *Phys. Rev. Lett.* **48**, 874 (1982).